The paper was published in the proceedings of the 11th International Conference on Physical Modelling in Geotechnics (ICPMG2026) and was edited by Ioannis Anastasopoulos. The conference was held from June 8th to June 12th 2026 in Zurich, Switzerland.

Proceedings of the 11th ICPMG 2026
11th International Conference on Physical Modelling in Geotechnics
8-12 June 2026, Zurich, Switzerland

The brittle response of axially-loaded piles: Physical models for teaching

A.H. Bateman, D.J. White
University of Southampton, UK, a.bateman@soton.ac.uk, david.white@soton.ac.uk

ABSTRACT: The load-displacement response of axially-loaded piles is controlled by the axial stiffness of the pile and the shaft friction t-z load transfer behaviour. In many soils, the t-z response softens beyond a peak value, sometimes to as low as 10% of the peak resistance. This behaviour can be critical to the design of offshore piles, particularly in rock. The t-z brittleness causes progressive failure that affects the peak axial capacity of the pile. This paper describes a set of physical models that demonstrate this effect in a simple way, with visual and quantitative demonstrations of the effect of t-z softening and pile axial stiffness on axial capacity. The models use dry spaghetti in three-point bending to provide a linear-elastic – brittle-softening t-z response. These pasta t-z elements are loaded in series via 3D-printed model piles with a range of axial stiffness. The response of this physical model can be simulated via classical pile solutions as well as by discrete modelling of the system of springs made up of the pasta t-z elements and the model pile. These physical models provide a visual demonstration of the progressive failure mechanism as well as quantitative results that match theoretical pile t-z response models. Combined with the accompanying teaching materials, these models provide a popular and insightful component of a masters-level course on advanced geotechnical engineering.

1 INTRODUCTION

The axial response of piles is a controlling factor in the design of foundations for onshore and offshore structures (Randolph and Gourvenec 2011), and consequently, forms an important topic in geotechnical engineering education.

In university courses and associated textbooks (e.g., Salgado 2022), the axial response of piles is generally divided into two components: (i) the ultimate capacity, and (ii) the elastic (serviceability) response. Current pile design methods for capacity and stiffness usually include elements of empiricism (Randolph 2003), with key parameters often calibrated based on load test databases, reflecting the difficulty in precisely calculating the pile response as a result of installation and loading. Despite this, it is important that the teaching process conveys the key mechanisms by which piles respond to load and shows how the mechanisms are controlled by the pile and pile-soil interaction parameters.

To simplify the three-dimensional pile problem and model the pile response, Seed and Reese (1957) and Coyle and Reese (1966) introduced the modelling of local load-displacement (t-z) curves along the pile shaft. These early t-z concepts have evolved through the development of analytical elastic t-z curves (Randolph and Wroth 1978) and the inclusion of soil non-linearity (e.g., Kraft et al. 1981, Bateman et al. 2022). A key aspect of t-z curves is their ability to represent progressive pile failure under axial load, which is modelled by the softening of the t-z curve (Randolph 2013). A softening t-z response of the form typically seen for drilled and grouted piles embedded in rock is shown in **Error! Reference source not found.**.

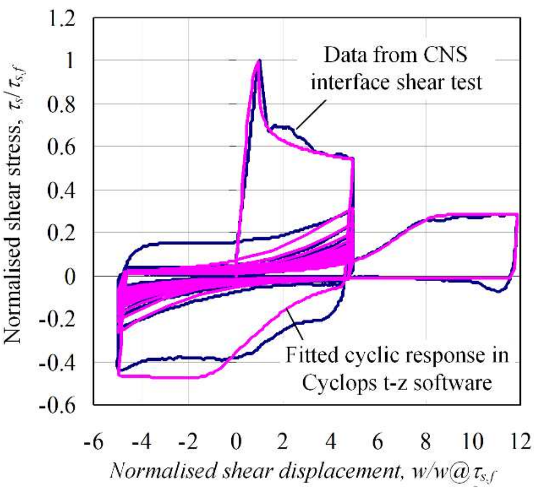

Figure 1. Typical t-z softening response of a pile element (Randolph & White 2008)

In this case, under monotonic loading, the shaft shear stress on a pile element falls by a factor of 2. A further fall in capacity is evident during subsequent cyclic loading. Similar forms of softening t-z response are found in clays, with guidelines typically suggesting a fall to 70% of the peak capacity (ISO 2025). In rock, the fall in capacity can be more significant, depending on the pile and rock parameters (e.g. Seidel and Haberfield 2002, Erbrich et al. 2010).

Any level of t-z softening, combined with the compression of the pile under axial loading, leads to a form of progressive failure, because the peak in load transfer cannot be mobilised simultaneously along the entire pile length. This mechanism is illustrated in **Error! Reference source not found.**. When the peak in resistance is mobilised at the central part of the pile (marked B), the upper section (A) has already displaced beyond the peak, while the lower part (C) is yet to mobilise the peak, due to axial shortening of the pile.

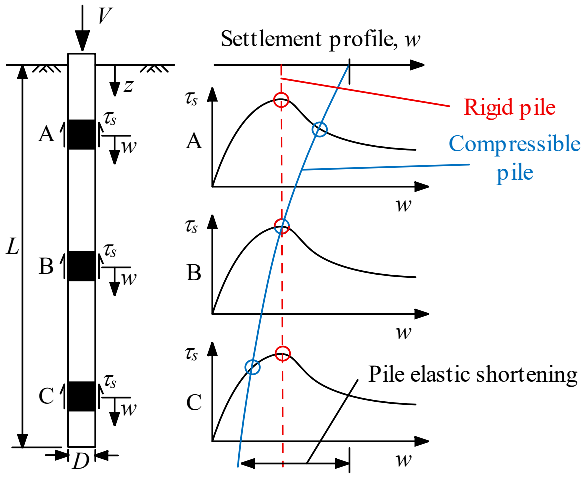

Figure 2. Illustration of progressive failure due to t-z softening (after Randolph & Gourvenec 2011)

The effect of this progressive failure mechanism on the axial pile capacity V_{max} can be quantified by the ratio parameter:

$$R_{pf} = V_{max}/V_{rigid} \tag{1}$$

which denotes the proportion of the 'ideal' or rigid pile capacity, V_{rigid}, that is mobilised under the maximum monotonic load, V_{max}. The example pile head response shown in **Error! Reference source not found.** is for a typical offshore drilled and grouted pile, and shows that only 64% of V_{rigid}, the 'ideal' capacity, is available under monotonic loading ($R_{pf} = 0.64$). This demonstrates the significance of progressive failure and shows the importance of teaching this mechanism, alongside methods for estimating both the ideal capacity of the pile and the pile head stiffness under working loads.

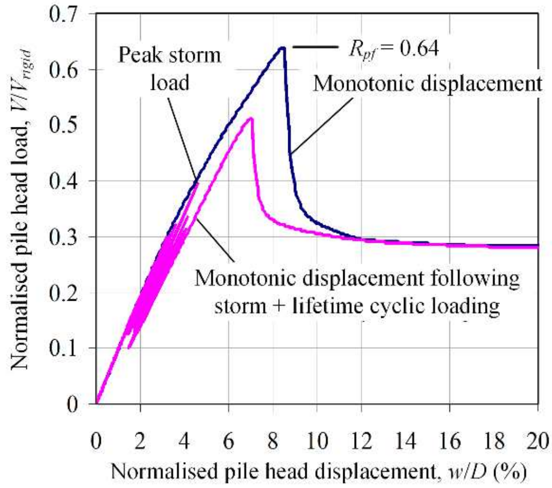

Figure 3. Pile head response with t-z softening (Randolph & White 2008)

To this end, the purpose of this paper is to describe the design and theoretical analysis of a physical model that demonstrates the progressive failure effect using dry pasta as a simple mechanical analogue for the pile-soil interaction. The paper structure is as follows:

1. Theoretical models for pile response are described, illustrating the concepts that are covered in the teaching of axial pile behaviour.
2. The mechanical analogue system for pile-soil interaction, based on dry pasta, is introduced.
3. The performance of the resulting desktop model of axial pile behaviour is evaluated, showing that it captures the key underlying mechanisms.
4. The associated teaching material is described, showing how the physical models fit into teaching activities at the University of Southampton.

2 THEORETICAL MODELS

2.1 General elastic axial pile response

The axial response of a compressible pile under axial load is governed by the following expression, which combines the pile elastic compression with the equilibrium of a thin pile element of height dz:

$$\frac{d^2w}{dz^2} = \frac{1}{(EA)_p}\frac{dF}{dz} \tag{2}$$

where w is the axial movement of a pile element at depth, z, $(EA)_p$ is the pile axial stiffness, and F is the axial force in the pile (which is denoted V at the pile head). For a cylindrical pile, the axial load in the pile varies due to load transfer, t, via shear stress, τ_s, on the pile shaft around the circumference πD, such that:

$$\frac{dF}{dz} = -t = -\pi D \tau_s \quad (3)$$

The t-z stiffness can be defined using the ratio of load transfer to axial pile movement, $k_t = t/w$.

2.1.1 Elastic solution for pile head response

In conditions where the soil properties are constant with depth, integration of the governing equation of the pile response leads to a general expression for the pile head stiffness (Mylonakis and Gazetas 1998):

$$K_{head} = \frac{V}{w_{head}} = S\frac{k_Q + S\tanh(\mu L)}{S + k_Q\tanh(\mu L)} \quad (4)$$

where $\mu L = \sqrt{\frac{k_t}{(EA)_p}} L$, $S = \frac{(EA)_p}{L}\mu L = \sqrt{(EA)_p k_t}$ and w_{head} is the settlement at the pile head, L is the pile length and k_Q is the stiffness of the pile base. For a long pile, the contribution of the base response may be negligible (and $\tanh(\mu L) \to 1$), so:

$$K_{head} = \frac{V}{w_{head}} = S = \sqrt{(EA)_p k_t} \quad (5)$$

2.1.2 Theoretical solution for t-z response

The elastic load transfer stiffness k_t is controlled by the shear modulus of the surrounding soil, G. Theoretical solutions involving integration of the shear stresses in the surrounding soil are presented by Randolph & Wroth (1978), and show that:

$$k_t = \frac{2\pi}{\zeta} G \quad \text{where} \quad \zeta \approx ln\left(\frac{2L}{D}\right) \approx 4 \quad (6)$$

Equations (5) and (6) provide simple solutions that allow the elastic axial head stiffness of an axially-compressible pile to be estimated, but neglect any post-peak behaviour.

2.2 General solutions for brittle pile capacity

Any softening (brittleness) in the t-z response leads to a capacity reduction for a compressible pile, so that $R_{pf} < 1$. Solutions for R_{pf} based on idealised forms of t-z response are presented by Murff (1980) and Randolph (1983) using the t-z responses in **Error! Reference source not found.**.

The Murff (1980) analysis combines an initial elastic response (Equation 6) with a subsequent constant 'residual' plastic resistance, defined as a proportion of the peak shear stress value $\tau_{s,f}$, i.e. $\xi = \tau_s/\tau_{s,f}$. Randolph (1983) used a non-linear response for the pre- and post-peak responses, characterised by the displacement to the residual value, Δw_{res}.

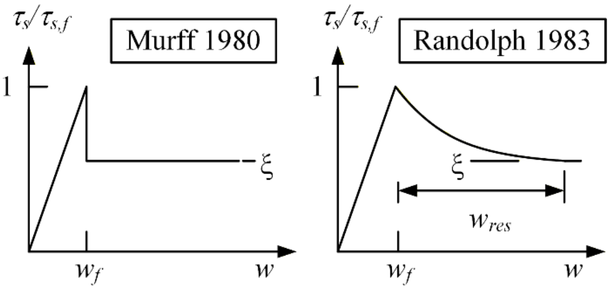

Figure 4. Idealised models for brittle t-z response

Both the Murff (1980) and Randolph (1983) approaches lead to solutions for R_{pf} that depend on the t-z brittleness and the pile shortening. The shortening depends on the total peak friction along the pile and the pile axial stiffness. These parameters are captured in the pile compliance, C, defined as:

$$C = \frac{Q_s L}{(EA)_p w_r} = \frac{\pi D \tau_{s,f} L^2}{(EA)_p w_r} = (\mu L)^2 \left(\frac{w_f}{w_r}\right) \quad (7)$$

where Q_s is the maximum shaft friction mobilised on a rigid pile and w_r is the displacement at which the residual stress is reached ($w_r = w_f + \Delta w_{res}$ in Randolph 1983, $w_r = w_f$ in Murff 1980).

The resulting variation in R_{pf} with compliance, C, is illustrated in **Error! Reference source not found.** based on (i) the analytical solution fitted by Randolph (2013) to the earlier numerical studies (Randolph 1983) given by Equation 8 and (ii) the Murff (1980) solution for the linear elastic-brittle response given by Equation 9. While the Randolph (2013) solution is based on a sophisticated non-linear t-z model, the Murff (1980) solution with $\xi = 0$ is focused on in this paper because it closely represents the physical model described later.

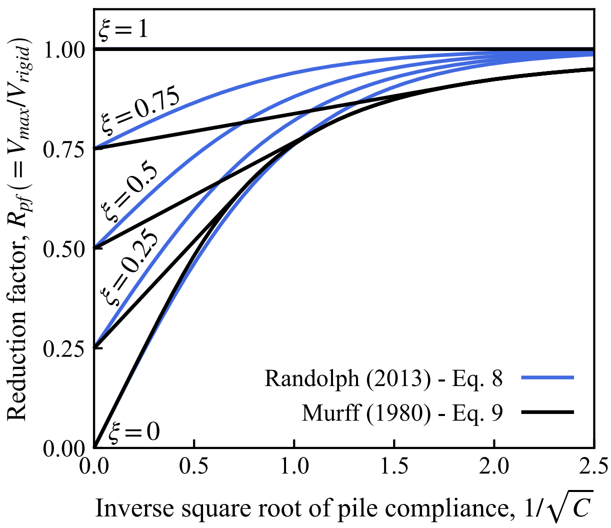

Figure 5. Reduction factor, R_{pf} from progressive failure

$$R_{pf} \approx \xi + (1-\xi)\tanh\left(\frac{1}{\sqrt{C}}\right) \quad (8)$$

$$R_{pf} = \xi\frac{L_p}{L} - \frac{1}{\sqrt{C}}\left[\frac{\alpha\exp\left(-2\left(1-\frac{L_p}{L}\right)\sqrt{C}\right)+1}{\alpha\exp\left(-2\left(1-\frac{L_p}{L}\right)\sqrt{C}\right)-1}\right] \quad (9)$$

where $\frac{L_p}{L} = 1 + \frac{1}{2\sqrt{C}}\ln\left[\frac{1}{\alpha}\left(1-\frac{2}{\xi}+\frac{2}{\xi}\sqrt{1-\xi}\right)\right]$

$$\alpha = \frac{-\sqrt{C}+k_Q L/(EA)_p}{\sqrt{C}+k_Q L/(EA)_p}$$

The ratio L_p/L represents the normalised depth to which t-z yield has progressed, and is limited to between 0 and 1 when input into Equation 9.

2.3 Discrete spring model for pile response

An analysis of the pile response can also be developed based on a finite number of discrete springs, akin to the schematic in Figure 6. This leads to the same trends as described above and directly represents the physical model described later.

The pile head stiffness can be computed using the discrete spring formation shown in Figure 6. Firstly, the elastic stiffness of the individual pile springs is:

$$k_p = N\frac{EA}{L} \quad (10)$$

where N is the number of pile springs.

From which a recursive formulation can be used to compute the pile head stiffness, k_{head}:

$$k(0) = k_Q \quad (11a)$$

$$k(n) = k_t\Delta z + \left(\frac{1}{k(n-1)}+\frac{1}{k_p}\right)^{-1} \quad (11b)$$

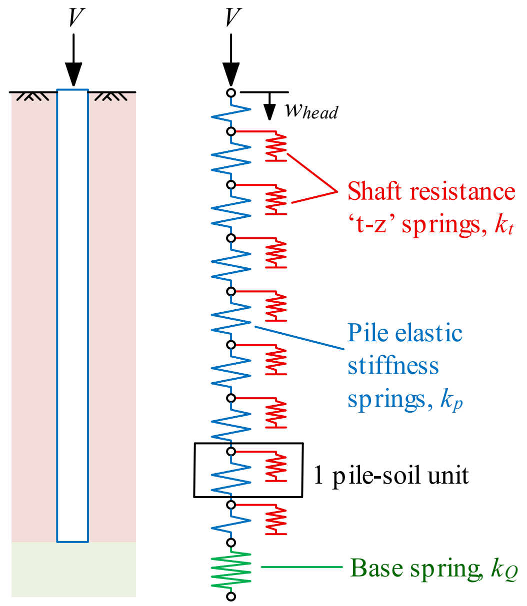

Figure 6. Elastic axially-loaded pile-soil system

where $n = 1, 2, 3, \ldots, N$ refers to the pile-soil stiffness below n pile-soil units (Figure 6), k_Q is the stiffness of the base spring (taken here as 0), Δz is the length of the pile shaft that the t-z curve represents and $k(N) = k_{head}$. k_t can be given by Equation 6.

The Murff (1980) brittle t-z response with $\xi = 0$ (**Error! Reference source not found.**) can be incorporated into this analysis by recognising that above the pile elevation where $w = w_f$ there is no t-z contribution, and the response is simply an elastic column, for which the stiffness is $(EA)_p$. A similar approach was used by Murff (1980) to develop an analytical solution to the brittle pile response. Therefore, to compute the pile head stiffness for the head displacement at which N_f t-z springs have exceeded w_f, Equation 11 can be employed for $n = 1, 2, 3, \ldots, (N-N_f)$ to calculate $k(N-N_f)$, which can be considered to be acting in series with the remaining pile springs. Therefore:

$$k_{head} = \left(\frac{1}{k(N-N_f)}+\frac{N_f}{k_p}\right)^{-1} \quad (12)$$

Using Equations 10, 11 and 12, the force-displacement response at the pile head is plotted in Figure 7 for different values of N for an example pile.

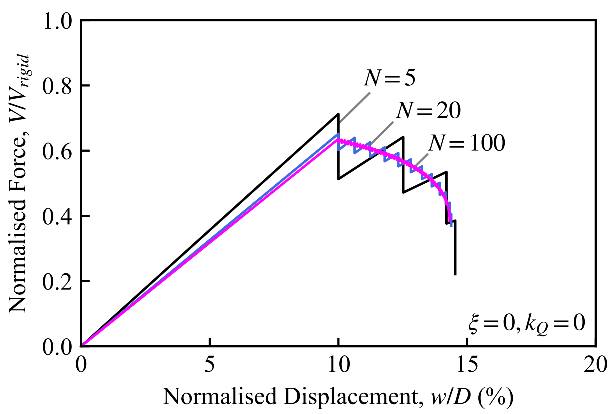

Figure 7. Normalised load-displacement curve using varying numbers of discrete springs, N

This approach can be used to identify the number of springs required to achieve a sufficiently smooth head response. For example, with only two t-z springs, the pile head load must fall by at least a factor of 2 when the upper t-z spring fails, because the lower spring must be mobilising a lower load at that point (due to its lower displacement, from compression of the pile). Also, for $N = 5$, only 4 distinct t-z failure locations can be seen since the lowest (final) two t-z elements fail simultaneously. A similar effect can be seen with higher N values. The calculated head response is smoother when a higher number of springs N is used and with increasing μL.

3 PASTA-BASED T-Z ANALOGUE

To support teaching of pile behaviour at the University of Southampton, a 3D printed model pile system using a pasta-based brittle t-z analogue has been developed. This demonstrates the progressive failure mechanism that influences axial pile design and enables students to develop an intuitive understanding of t-z curves and pile-soil interaction.

The complete physical model of the pile-soil system is comprised of a 3D printed model pile supported by multiple spaghetti t-z elements, all held within a support frame (Figure 8). This system behaves similarly to the discrete spring model.

3.1 Model pile

The pile is constrained to move freely in the vertical direction within a guide in the back plate of the support frame. Rigid and compressible versions of the model pile allow comparison of behaviour with and without the progressive failure mechanism. The compressible pile features alternating linear springs and spaghetti supports, repeating each 20 mm.

Both the piles and the support frame are 3D printed as single parts (Figure 9), in a horizontal orientation on the print bed. No print support elements are required, meaning that the components can be used immediately on completion of printing, without any further finishing required. This is achieved by limiting overhang angles and using a square cross-section for the pile.

The pile and support frame designs are modular, allowing larger and smaller versions to be produced, with different numbers of t-z springs, varying pile compressibility and different lengths of spaghetti. The example model pile shown in Figure 8 has eight pile springs ($N = 8$), each with a measured stiffness of $k_p \approx 11$ N/mm.

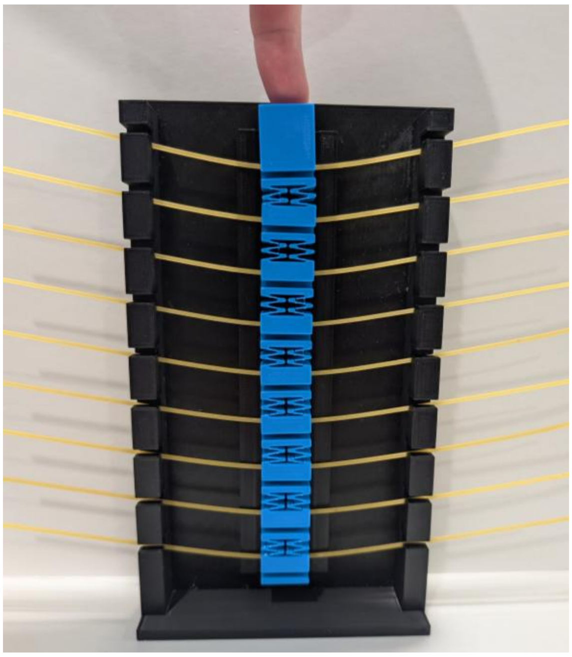

Figure 8. Photograph of pile system during loading.

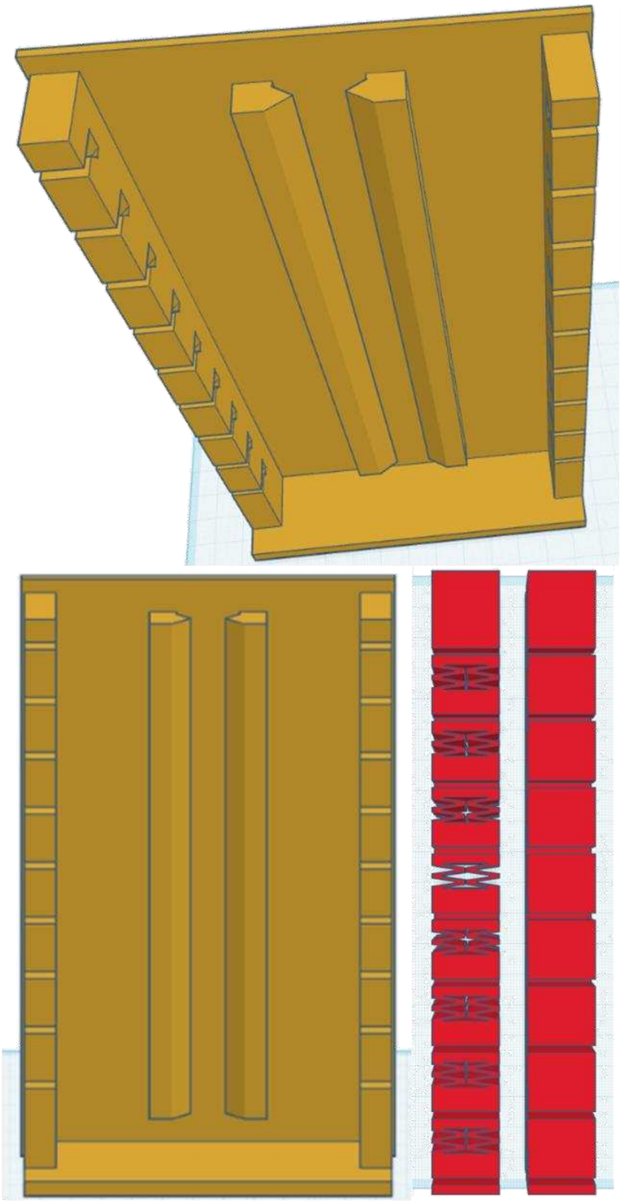

Figure 9. CAD model of support frame and piles.

3.2 Spaghetti t-z model

Dry spaghetti is used to produce a brittle t-z response. Pillars on each side of the back plate support the spaghetti which, in turn, support the pile at the centre of their span. The supports are located 100 mm apart. This system loads each piece of spaghetti in three-point bending. Each pillar contains knife-edge features that support the spaghetti which are equally spaced vertically. Similar knife edge features are incorporated at the same vertical spacing within the model piles. Slots allow the spaghetti to be placed into the front of the model while it is laid flat, rather than needing to be threaded through the supports.

The spaghetti resembles, conceptually, the horizontal strata of soil, loaded downwards by the model pile. The deformation pattern in three-point bending is different to the pattern of downdrag associated with the elastic t-z solution, but the similarity is sufficient as a mechanical analogue.

To analyse this model, two parts of the *t-z* curve are required: (1) the initial stiffness and (2) the failure displacement. Firstly, in three-point bending, with loading at the centre, the stiffness of each spaghetti pasta is:

$$\frac{\Delta F}{w} = \frac{48EI}{L_s^3} \tag{13}$$

where ΔF is the vertical force transfer between the pile and the spaghetti, w is both the settlement of the pile at that elevation and the midspan deflection of the spaghetti, E is the Young's modulus of the spaghetti, I is the moment of inertia ($I = \pi D_s^4/64$) and L_s is the horizontal distance that the spaghetti spans between supports. If the vertical spacing between the spaghetti springs is Δz, then the beam stiffness is equivalent to a load transfer stiffness, k_t:

$$k_t = \frac{1}{\Delta z}\frac{\Delta F}{w} = \frac{48EI}{\Delta z\, L_s^3} \tag{14}$$

Secondly, each spaghetti in the model (under three-point bending) will fail at the failure displacement:

$$w_f = \frac{L_s^2 \sigma_f}{6\mathrm{E}D_s} \tag{15}$$

where σ_f is the flexural stress at failure and D_s is the diameter of the spaghetti.

Spaghetti properties (E and σ_f) required in these two equations were determined from a three-point bending (3PB) tests on single spaghetti pasta conducted for this study. As expected, the spaghetti was found to be an elastic-perfectly brittle material. From the maximum load at failure, ΔF_f, the flexural stress at failure of the spaghetti is given by:

$$\sigma_f = \frac{8L_s}{\pi D_s^3}\Delta F_f \tag{16}$$

where L_s is the distance between supports and ΔF_f is the force measured at failure. This, alongside the failure displacement, w_f, is used to estimate the Young's modulus:

$$E = \frac{L_s^2 \sigma_f}{6 w_f D_s} \tag{17}$$

The measured properties of dry spaghetti are compared with typical properties from the literature in **Error! Reference source not found.** (e.g., Voisey and Waski 1978, Vemareddy et al 2021). Notably, the measured results are quite variable, by at least a factor of 2, despite using spaghetti from a single packet.

Table 1. Properties of dry spaghetti pasta

Property	Typical (literature)	Measured (this study)
Young's modulus, $\boldsymbol{E}$	$5-20$ GPa	$4-11$ GPa
Flexural failure stress, $\boldsymbol{\sigma_f}$	100 N/mm^2	$25-50$ N/mm^2
Diameter, $\boldsymbol{D_s}$	1-2 mm	1.6 - 1.7 mm

A loading stiffness range (from three-point bending) of $\Delta F/w = k_t \Delta z = 0.08 - 0.2$ N/mm was measured. This is ~ 100 times smaller than the model pile stiffness calculated in Section 3.1. Given a vertical spacing of $\Delta z = 20$ mm, the load transfer stiffness is $k_t = 4 \times 10^{-3} - 1 \times 10^{-2}$ N/mm^2. The measured values for w_f are between 4 and 10 mm.

The tests for this study showed there is wide variation in spaghetti properties which may affect the model response. Rather than detracting from the teaching value of the model, this actually adds to the analogy by reflecting real geotechnical variability.

3.3 Rigid model pile response

The rigid pile capacity, for a model with 9 spaghetti t-z springs shown in Figure 8 (i.e., with a spaghetti also acting as the base spring), is given by:

$$V_{rigid} = (N+1)\,\Delta F_f = (\mathrm{N}+1)\frac{\pi D_s^3}{8 L_s}\sigma_f \quad (18)$$

From the measured spaghetti properties (**Error! Reference source not found.**), this would yield a predicted range of $V_{rigid} = Q_s = 4-8$ N or $\approx 400-800$ grams and a failure settlement of $w_f = 4-10$ mm ($L_s = 100$ mm, **Error! Reference source not found.**).

3.4 Flexible model pile response

Given k_p, $k_t \Delta z$ (Equation 14) and $k_Q = k_t \Delta z$, the overall head stiffness of the flexible model pile can be calculated using the recursive Equations 11 and 12, following the discrete spring model approach. The tendency for progressive failure can also be expressed in the form of the pile compliance:

$$C = \frac{Q_s}{w_r}\left(\frac{N}{k_p}\right) \quad (19)$$

The predicted load-displacement curve is illustrated in black in **Error! Reference source not found.** (with associated spaghetti parameters provided), where it can be seen that $C = 1.26$ and $R_{pf} = 0.74$ (only 4.5% higher than that predicted by Murff 1980). This model predicts the first spaghetti fails at 4.5 mm of head displacement and the final three spaghetti fail simultaneously. Displacement-controlled loading (or a steady hand) is needed for controlled observation of the progressive failure since the head load decreases after each spaghetti fails.

The physical model has also been tested using a displacement-controlled actuator to provide a comparison with the theoretical approach presented. The obtained load-displacement curve is shown in blue in **Error! Reference source not found.**. This measured result is a good match to the predicted line calculated above.

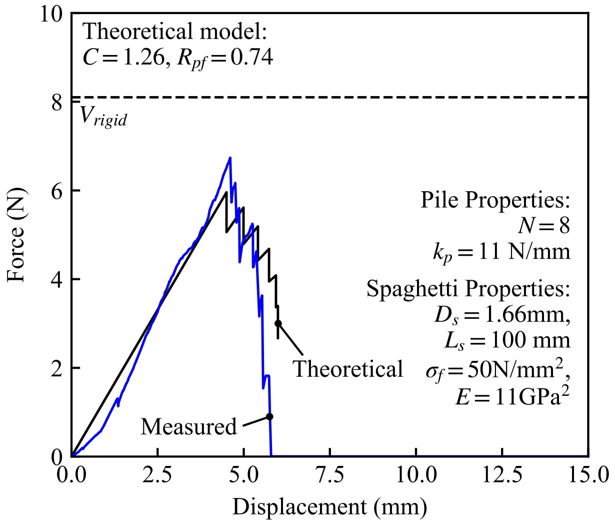

Figure 10. Pile head response – measured and calculated

3.5 Qualitative observations

The qualitative response of the system is illustrated by the photo shown in Figure 8. The loading can be applied by hand, steadily displacing the top of the pile downwards. It is visually clear that the spaghetti near the top of the pile deflects more than at the bottom, due to axial compression of the pile. It is also visible (and audible) when the strands of spaghetti fail in sequence. These follow a general pattern from the top downwards, but due to variability in the diameter and strength of the spaghetti, it is rare that all nine spaghetti fail in perfect sequence from top to bottom.

Using two models, one with a rigid pile and one compressible, it is possible to feel the difference in both pile head stiffness (without failing any spaghetti) and also the peak capacity, by testing the two models simultaneously or in quick succession.

These demonstrations can be performed by students during a class, on individual models that they assemble themselves. It can also be performed as a demonstration at the front of the class, with commentary and explanation by the lecturer. The model can operate when oriented vertically or laid horizontally under a classroom visualiser.

4 ASSOCIATED TEACHING MATERIAL

These physical models are used in the teaching of module CENV6122 Advanced Geotechnical Engineering at the University of Southampton. This is an optional module at Level 6 in the MEng and MSc Civil Engineering programs. A different topic is tackled during each week of the 12-week semester, with four topics dedicated to piling engineering.

Topic J is the axial load-settlement response of piles. The course is delivered using a flipped classroom approach. The students watch a short set of prerecorded videos that cover the course content. The face-to-face sessions are referred to as 'Lectorials', being a hybrid of a lecture and a tutorial.

During the two-hour Lectorial on pile settlement, the students complete a worksheet that begins with simple calculations of elastic pile stiffness. This is followed by a mini-lecture recapping and extending the coverage of progressive failure due to pile brittleness. The physical models are then used to visualise the underlying mechanism, and the students estimate the level of progressive failure in both the physical models and the two practical case studies. These case studies are:

1. The design of driven tubular piles loaded in tension for a floating bridge on the Norwegian E39 coastal highway. This activity uses publicly-available ground investigation data and a bridge concept design.
2. The design of grouted piles in rock, to anchor a tension leg platform installed for a wind farm in the UK's Celtic Sea region.

For each case study, the students perform simple analytical calculations to estimate the effect of progressive failure. They then complete a numerical analysis using the RATZ t-z software (provided courtesy of Prof. Mark Randolph) to quantify the progressive failure in more detail.

5 CONCLUSIONS

The load-displacement response of axially-loaded piles is a soil-structure interaction problem controlled by the axial stiffness of the pile and the shaft friction t-z load transfer. In many soils the t-z response softens beyond a peak value. In soft rocks, the resistance can fall by a factor of 2 or more. This t-z brittleness causes progressive failure that affects the peak axial capacity of the pile. This mechanism should be covered when teaching pile axial capacity, even though the detail of the t-z softening is an advanced subject.

This paper shows a physical modelling approach that meets this aim in a simple way, with visual and quantitative demonstrations of the effect of t-z softening and pile axial stiffness on axial capacity. The models have the following features:

1. A representation of pile-soil interaction at multiple levels down a set of model piles that have different controlled axial stiffnesses.
2. A simple mechanical system based on three-point bending of dry spaghetti, which provides a brittle t-z response.

The behaviour of the models is consistent with the axial pile response predicted by classical analysis using brittle t-z models. The progressive failure mechanism is visible as the physical model is loaded, and the reduction in capacity can be quantified. The capacity varies with the relative stiffness of the pile-soil system and the t-z brittleness, and the resulting level of progressive failure is consistent with published solutions. The resources to manufacture the components of the physical model by 3D printing are available from the lead author's github site.

ACKNOWLEDGEMENTS

Both authors acknowledge support from the EPSRC Supergen Offshore Renewable Energy Hub (grant EP/Y016297/1). We thank Prof,. Mark Randolph for generously providing his RATZ software for use in teaching.

REFERENCES

Bateman, A.H., Crispin, J.J., Vardanega, P.J., and Mylonakis, G. (2022). Theoretical t-z curves for axially loaded piles. *Journal of Geotechnical and Geoenvironmental Engineering, ASCE*, 148(7): 04022052. doi:10/h7th.

Coyle, H.M., and Reese, L.C. (1966). Load transfer for axially loaded piles in clay. *Journal of the Soil Mechanics and Foundations Division, ASCE*, 92(2): 1–26. doi:10.1061/jsfeaq.0000850.

Erbrich, C.T., O'Neill, M.P., Clancy, P., and Randolph, M.F. (2010). Axial and lateral pile design in carbonate soils. In *Proc. 2nd Int. Symp. on Frontiers in Offshore Geotechnics, ISFOG 2010*, Perth, Australia.

ISO (2025) Standard 19901-4: Oil and gas industries including lower carbon energy — Specific requirements for offshore structures Part 4: Geotechnical design considerations. International Standardisation Organisation.

Kraft, L.M., Ray, R.P., and Kagawa, T. (1981). Theoretical t-z curves. *Journal of the Geotechnical Engineering*

Division, ASCE, 107(11): 1543–1561. doi:10.1061/ajgeb6.0001207.

Murff, J.D. (1980). Pile capacity in a softening soil. *International Journal for Numerical and Analytical Methods in Geomechanics*, 4(2): 185–189. doi:10.1002/nag.1610040208.

Mylonakis, G., and Gazetas, G. (1998). Settlement and additional internal forces of grouped piles in layered soil. *Géotechnique*, 48(1): 55–72. doi:10.1680/geot.1998.48.1.55.

Randolph, M.F. (1983). Design considerations for offshore piles. In *Conference on Geotechnical Practice in Offshore Engineering*, Austin, Texas.

Randolph, M.F. (2003). Science and empiricism in pile foundation design. *Géotechnique*, 53(10): 847–875. doi:10.1680/geot.2003.53.10.847.

Randolph, M.F. (2013). McClelland Lecture: Analytical contributions to offshore geotechnical engineering. In *Proceedings of the 18th International Conference on Soil Mechanics and Geotechnical Engineering*, Paris.

Randolph, M., and Gourvenec, S. (2011). *Offshore Geotechnical Engineering*. CRC Press.

Randolph, M.F., and White, D.J. (2008). Offshore foundation design - A moving target. In *Foundations: Proceedings of the Second BGA International Conference on Foundations*, ICOF2008.

Randolph, M.F., and Wroth, C.P. (1978). Analysis of deformation of vertically loaded piles. *Journal of the Geotechnical Engineering Division, ASCE*, 104(12): 1465–1488. doi:10.1061/ajgeb6.0000729.

Salgado, R. (2022). *The Engineering of Foundations, Slopes and Retaining Structures*. 2nd edition. CRC Press.

Seed, H.B., and Reese, L.C. (1957). The action of soft clay along friction piles. *Transactions, ASCE*, 122(1): 731–754. doi:10.1061/taceat.0007501.

Seidel, J.P. and Haberfield C.M. (2002). A theoretical model for rock joints subjected to constant normal stiffness direct shear. *International Journal of Rock Mechanics and Mining Sciences* 39(5):539-553

Vemareddy, M., Bandhari, S. and Gollamundi, P. (2021). Estimating the Young's Modulus of spaghetti with a buckling experiment. Journal of Emerging Investigators. 5: 1-4.

Voisey, P.W. and Wasik, R. (1978). Measuring the Strength of Uncooked Spaghetti by the Bending Test. *Canadian Institute of Food Science and Technology Journal*, 11(1): 34–37. doi:10.1016/S0315-5463(78)73157-3.